SCIENTIFIC REPORTS

OPEN

SUBJECT AREAS:
SYNTHESIS OF GRAPHENE
CHEMISTRY
MATERIALS CHEMISTRY
MATERIALS SCIENCE

Received
1 July 2013

Accepted
16 January 2014

Published
5 February 2014

Correspondence and requests for materials should be addressed to H.L. (Hong-lin@mail.tsinghua.edu.cn)

Low temperature reduction of free-standing graphene oxide papers with metal iodides for ultrahigh bulk conductivity

Chenyang Liu[1], Feng Hao[1], Xiaochong Zhao[1,2], Qiancheng Zhao[1], Songping Luo[1] & Hong Lin[1]

[1]State Key Laboratory of New Ceramics & Fine Processing, School of Materials Science and Engineering, Tsinghua University, Beijing 100084, China, [2]Science and Technology on Surface Physics and Chemisty laboratory, Mianyang, 621907, China.

Here we report a green and facile route for highly efficient reduction of free-standing graphene oxide (GO) papers with metal iodide aqueous solutions at low cost. The metal iodides (MgI_2, AlI_3, ZnI_2, FeI_2) were synthesized directly from metal and iodine powder with water as a catalyzer. An extremely high bulk conductivity of 55088 S/m for reduced graphene oxide (rGO) papers were obtained with FeI_2 solution of which pH = 0 at 95°C for 6 hours. The catalytic effect of strong Lewis acid for the promotion of the nucleophilic substitution reaction is responsible for the greatly improved bulk conductivity. Furthermore, it was found that the layer-to-layer distance (d_L) and the crystallinity of the rGO papers are regarded as two main factors affecting the bulk conductivity rather than C/O ratio and defect concentration.

Graphene has attracted much attention[1–5] due to its unique properties, such as extremely high conductivity, excellent mechanical properties and room temperature quantum Hall effect, which can be used in many electronic devices such as solar cells[6,7], supercapacitors[8–10] and field effect transistor[11]. Among all graphene-based materials, free-standing graphene papers, in the form of multilayered graphene sheets, have been proved to be easily applied into potential commercial applications[12,13]. In the past few years, many methods, such as micro mechanical exfoliation[14], chemical vapor disposition[15,16], chemical reduction of GO[17–26], have been developed to prepare single or few-layers rGO sheets. Among all these methods, chemical reduction of free-standing GO papers is regarded as a simple one-step process which is suitable for large scale production.

The basic route for chemical reduction of GO papers involves the oxidation of raw graphite, subsequent exfoliation of GO into individual GO sheets, the process of making GO sheets into GO papers, and the in-situ chemical reduction of GO papers to form rGO papers, among which the process of chemical reduction of GO papers plays a key role that dominates the final quality of the rGO papers. The resulting rGO papers can possess favorable properties, including good conductivity, catalytic property and reasonable mechanical strength, although structural defects are unavoidable during these processes.

Several reductive agents, such as hydrazine[17,18], hydrazine derivate[19], cellulose[20], sodium hydride[21], $NaBH_4$[22,23], HI[24,25], and AlI_3 ethanol solution[26] have been used to reduce GO. So far, rGO papers with the highest electrical conductivity of 29800 S/m was obtained by submerging GO papers into 55% HI solution for 1 h at 100°C[24], which was attributed to the nucleophilic substitution reaction of epoxy groups and hydroxyl groups by I^- and the promotion of the reaction by high concentration H^+. Meanwhile, the lowest binding energy of C-I among all the carbon–halogen bonds resulted in the spontaneous elimination of most iodine atoms from the rGO papers. However, the relative high cost, especially strong corrosion nature of HI limits its further application. AlI_3 ethanol solution provided a mild and environmentally benign reductive process[26]. The metal cation Al^{3+}, which is a strong Lewis acid, can also promote the nucleophilic substitution. Nevertheless, the bulk conductivity of 5320 S/m for rGO papers was limited by both the low solubility of AlI_3 in ethanol and the low boiling point of ethanol of 80°C. Therefore, improving the concentration of metal iodide and incorporation of the role of metal cations as strong Lewis acid in promoting the nucleophilic substitution reaction is simultaneously desirable for developing a green, mild and more efficient reductive agent. In the present paper, we report a green and fast synthetic route of metal iodide at low cost for highly efficient reduction of GO papers. Four kinds of metal iodides (MgI_2, AlI_3, ZnI_2, FeI_2) were synthesized directly from metal and iodine powder with water as a catalyzer at low cost. At the same time,

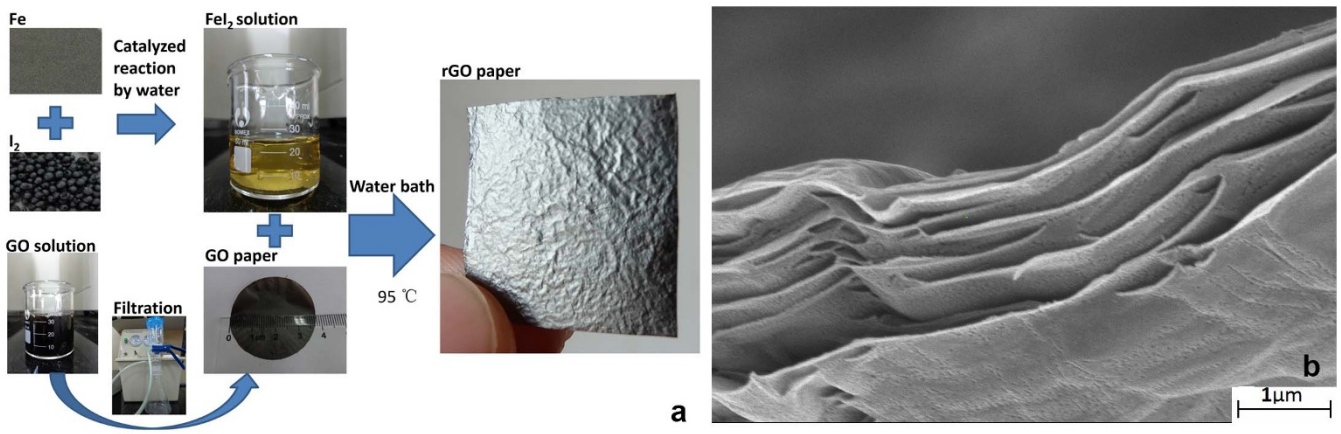

Figure 1 | Experimental procedures (a) and the SEM image of the cross section of the rGO paper (b).

aqueous hydrochloric acid (HCl) solution was introduced to tune pH values of these aqueous solutions to improve the reductive ability by inhibiting the hydrolysis of these strong Lewis acids. The effects of metal cations and pH values on the conductivity of rGO papers were investigated in detail. An extremely high bulk conductivity of 55088 S/m for rGO papers were obtained with FeI_2 solution of pH = 0 at 95°C for 6 hours.

Results

Reduction of GO paper by four kinds of metal iodide solutions. Fig. 1a shows the experimental procedure. The GO paper is in dark brown while the rGO paper is in grey with metal lustre, which indicates efficient reduction of the GO paper. Fig. 1b shows the SEM image of the cross section of the rGO paper (See more SEM images in Fig. S1 in supplementary information (SI)), of which the thickness is 1.3 μm. Meanwhile, the structure of rGO paper, which is composed of stacked rGO sheets, can be clearly observed in this figure. Fig. 2a shows the bulk conductivity, C/O ratio and I_D/I_G of the rGO papers reduced by the acidic aqueous solutions of different metal iodides with pH value of 1 and 2 (See detailed conductivity, C/O and I_D/I_G data in Table S1, Table S2 and Table S3 in SI. See detailed XPS and Raman spectra in Fig. S2 and Fig. S4 in SI). Firstly, for each metal iodide solution, lower pH value leads to higher bulk conductivity, which indicates that the presence of H^+ can inhibit hydrolysis of these strong Lewis acid to promote the nucleophilic substitution reaction of oxygen-containing groups by I^-. Secondly, the rGO papers reduced by different metal iodides show similar conductivity when pH = 1, indicating that these metal iodides show similar reductive ability. Furthermore, the rGO papers reduced by all the metal iodides at a pH of 1 exhibited bulk conductivities of higher than 30000 S/m, which is higher than the value of 29800 S/m by 55% HI solution[25], indicating that the strong Lewis acid plays a crucial role on the promotion of the nucleophilic substitution effects of I^-. Thirdly, even though the C/O ratio changes greatly as reductant changes when pH = 1, the conductivity stays almost the same. For instance, the C/O ratio of rGO paper reduced by MgI_2 is about 4 times of that of rGO paper reduced by AlI_3. Nevertheless, the conductivities of these rGO papers are almost the same, which clearly shows that high C/O ratio does not lead to high conductivity directly. Furthermore, the I_D/I_G slightly increases as the pH decreases for all the rGO papers, indicating the slight decrease of the defect concentration in rGO papers[27]. Fig. 2b and 2c shows the XRD patterns of the rGO papers reduced by the aqueous solutions of different metal iodides with pH value of 1 and 2, respectively. When pH = 1, rGO papers reduced by FeI_2, MgI_2 and ZnI_2 shows similar peak shape and peak position, while rGO paper reduced by AlI_3 shows a higher and left shifted peak compared with others, indicating that the rGO paper reduced by AlI_3 has better crystallinity and larger layer to layer distance (d_L). While better crystallinity leads to higher bulk conductivity, larger d_L may lead to lower bulk conductivity, which makes the rGO paper reduced by AlI_3 has comparable bulk conductivity with other rGO papers. Therefore, it seems that both d_L and crystallinity are decisive for conductivity of rGO papers. While these two factors change, the conductivity of rGO papers is decided by the compensation of those changes with each other. When pH = 2, the rGO papers reduced by FeI_2 shows comparable crystallinity but higher conductivity compared with rGO paper reduced by AlI_3, which can be attributed to larger d_L (left shifted peak) of rGO paper reduced by AlI_3. For the rGO papers reduced by MgI_2 and ZnI_2 when pH = 2, the conductivity is close to 0 S/m. The corresponding XRD patterns show two peaks, one is right shifted

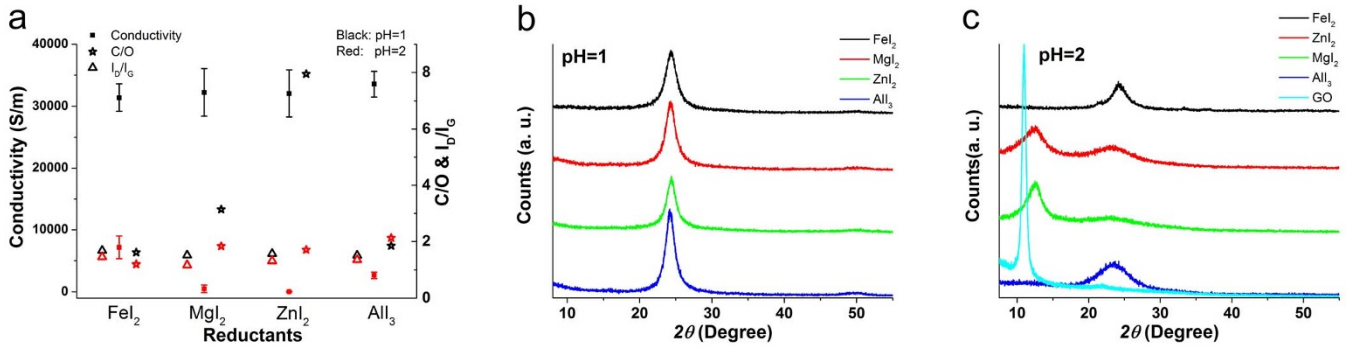

Figure 2 | The bulk conductivities, C/O ratio, I_D/I_G (a) and XRD patterns ((b). pH = 1, (c). pH = 2) of rGO papers reduced by the acidic aqueous solutions of different metal iodides.

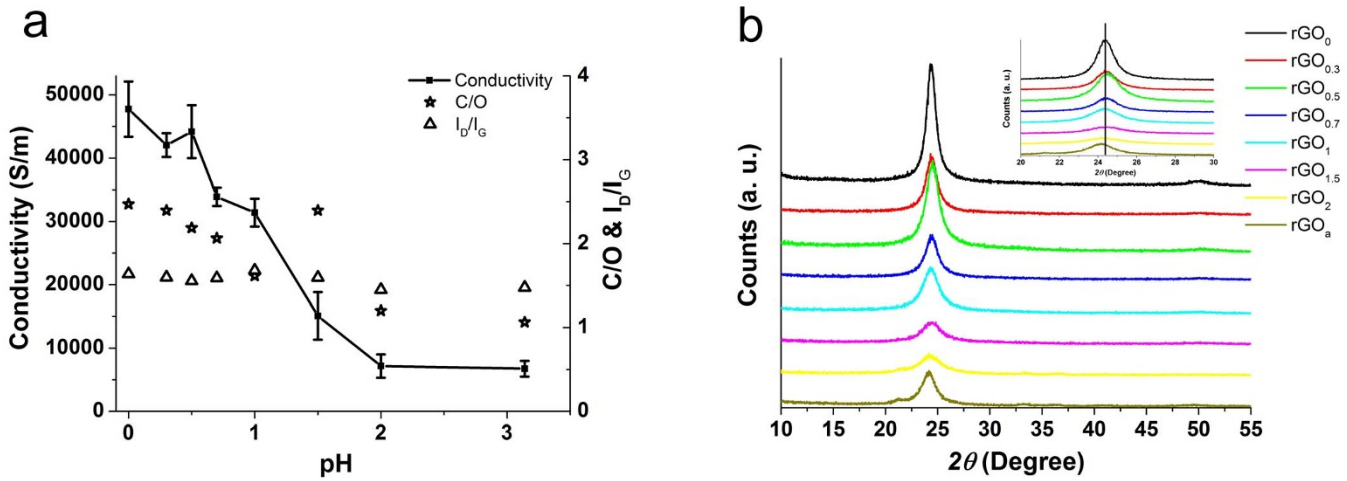

Figure 3 | The bulk conductivities, C/O ratio, I_D/I_G (a) and XRD patterns (b) of rGO papers reduced by FeI_2 solution with different pH.

GO peak and the other one is rGO peak. Such kind of XRD patterns indicate that the rGO papers reduced by MgI_2 and ZnI_2 are under intermediate state, that is, partially reduced GO and rGO exist simultaneously. From this result, the reduction process of GO can be indicated as follows. During the reduction, the crystallinity of GO paper is destroyed (lowering and widening XRD peak) and d_L decreases (right shifting XRD peak). Then, rGO gradually appears where the reaction proceeds fast and XRD peak corresponding to rGO starts to grow. Finally, all GO is reduced and the peak corresponding to GO disappears while the peak corresponding to rGO forms.

Summarizing the results above, both the magnitude of the conductance of rGO papers and the degree of reduction of GO papers can be well explained by the crystallinity and d_L rather than considering other factors, such as C/O ratio and defect concentration.

Reduction of GO by FeI_2 solution. The conductivity results mentioned above show that different cations lead to different reductive ability at different pH. The rGO papers reduced by FeI_2 solution demonstrate a high bulk conductivity at low concentration of H^+ (pH = 2), which implies that FeI_2 solution holds the potential of a next generation of highly efficient, mild and environmentally benign reductive agent. In the following, the effect of pH value on the reductive ability of FeI_2 solution was investigated in detail. Hereafter, rGO_x denotes the rGO papers reduced by FeI_2 solution at a pH of x, while rGO_a stands for the rGO paper reduced by as-made FeI_2 aqueous solution, of which pH = 3.16 due to hydrolysis effect. Fig. 3a shows that the bulk conductivity, C/O ratio and I_D/I_G of rGO papers reduced by FeI_2 aqueous solutions with different pH values. It can be seen that the bulk conductivity of rGO papers greatly increases as the pH value decreases, i.e., the concentration of H^+ increases. Moreover, the bulk conductivity becomes inert to the pH value when pH $\leq$ 0.5 and pH $\geq$ 2.0, indicating that the conductive ability of FeI_2 aqueous solution becomes inert to pH. Even though the pH is decisive to the conductivity of rGO papers, the I_D/I_G of rGO papers is insensitive to the change of pH while the C/O ratio changes randomly as the pH changes as discussed above. Fig. 3b shows that the crystallinity of rGO papers, which can be indicated from the peak intensity of the XRD pattern, increases as an inverse function of the pH value. However, d_L, which can be indicated from the peak position of the XRD pattern, reaches to a minimum when pH = 0.5. When further increase the solution pH value to over 0.5, the crystallinity turns to decrease while d_L starts to increase, resulting in a rapidly decreasing tendency of the bulk conductivity. It is important to mention that even though comparable high bulk conductivities are obtained for both rGO_0 and $rGO_{0.5}$, the reasons are different: the XRD results further confirm that the rGO_0 has the highest crystallinity while $rGO_{0.5}$ has the smallest d_L.

Discussion

Since Raman spectra (Fig. S4 in SI) show almost no change and C/O ratio changes randomly as pH changes, the d_L and crystallinity can be regarded as the main factors that affect the bulk conductivity of rGO papers due to the stacked structure of them[28]. Then the reasons for the changes of the crystallinity and d_L will be discussed in the following.

Fig. 4 shows the FTIR spectra of GO and rGO papers reduced by FeI_2 solution with different pH. The FTIR peaks of rGO_0 and $rGO_{0.3}$ at 1060 cm^{-1} and 1030 cm^{-1} are corresponding to alcoholic hydroxyl groups. While the peaks of $rGO_{0.5}$, rGO_1 and rGO_a appearing at 1220 cm^{-1} and 1560 cm^{-1} are corresponding to epoxy groups and deformed C-C bond due to the existence of epoxy groups, respectively[29]. Since for the epoxy groups, the oxygen atom is 0.19 nm above the carbon grid of rGO sheet while for alcoholic hydroxyl groups, the top hydrogen is 0.22 nm above the carbon grid[30], alcoholic hydroxyl groups are 0.03 nm "taller" than the epoxy groups. While rGO_0 and $rGO_{0.3}$ is rich in alcoholic hydroxyl groups and $rGO_{0.5}$ is rich in epoxy groups, the d_L of rGO_0 and $rGO_{0.3}$ is therefore larger than that of $rGO_{0.5}$. The deconvolution of carbon 1 s peaks in XPS patterns of the rGO papers reduced by FeI_2 solution

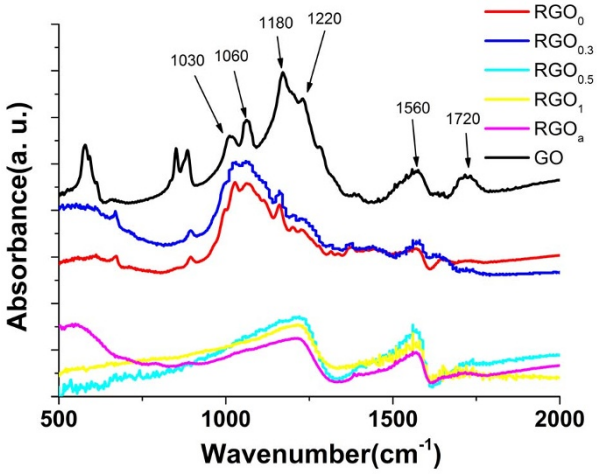

Figure 4 | FTIR spectra of GO and rGO papers reduced by FeI_2 solution with different pH.

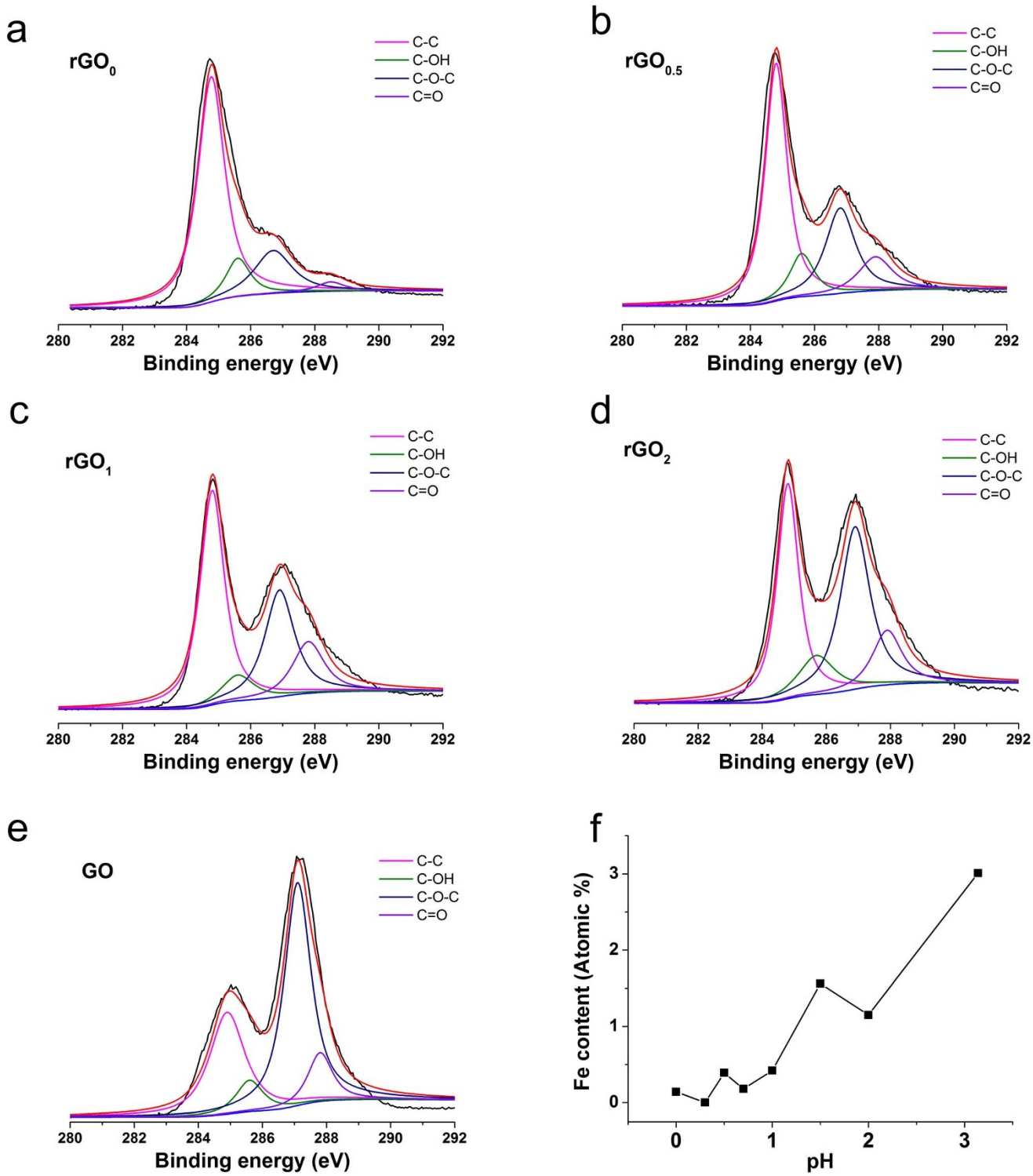

Figure 5 | Deconvolution of C 1 s peak of rGO papers reduced by FeI_2 solution with different pH (a ~ d) and GO paper (e) and relative content of Fe in each rGO paper (f). The position of C-C, C-OH, C-O-C and C=O is 284.8 ± 0.1 eV, 285.6 ± 0.1 eV, 286.9 ± 0.1 eV and 287.9 ± 0.1 eV, respectively.

with different pH values (Fig. 5 a ~ e) shows the same results as FTIR spectrums: as pH increases, the relative content of C-O-C increases while the relative content of C-OH decreases. Moreover, the relative content of residual Fe in rGO papers increases as pH increases (Fig. 5f). The elimination of alcoholic hydroxyl groups, the residual Fe in rGO papers and the existence of epoxy groups when pH ≥ 0.5 can all be attributed to the hydrolysis of Fe^{3+}, whose formation process is shown in equation 1. The hydrolysis process of Fe^{3+} is normally consisted of four steps[31]: (a) the formation of low molecular weight species, such as $FeOH^{2+}$, $Fe(OH)_2^{+}$ and $Fe_2(OH)_4^{2+}$ (Equation 2, 3 and 4, respectively). (b) The formation of red cationic polymer with a $Fe(O,OH,H_2O)_6$ octahedra structure, in which OH^-/Fe^{3+} ratio ranges from 2.5 to 3. (c). The aging of the polymer, with eventual conversion to oxide phase. (d). Precipitation directly from the low molecular weight molecules. The hydrolysis of Fe^{3+} will improve the affinity of Fe^{3+} with -OH group rather than

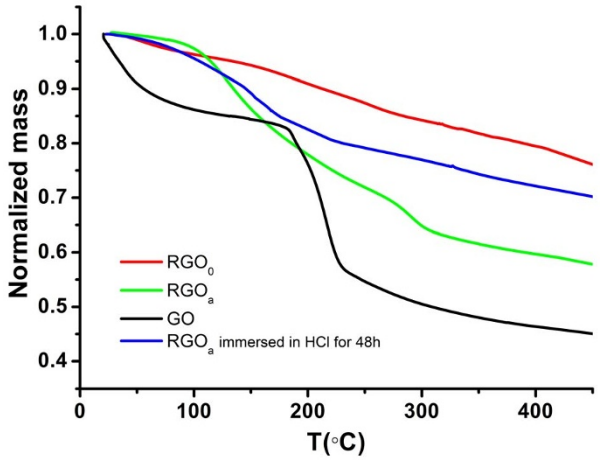

Figure 6 | TGA curves of rGO_0, rGO_a, rGO_a immersed in HCl for 48 h, and GO.

-C-O-C- group due to its tendency to form a series of hydrolysis products mentioned above and the decreased coordination ability of $FeOH^{2+}$, $Fe(OH)_2^{+}$ and $Fe_2(OH)_4^{2+}$ compared with Fe^{3+}. Therefore, the hydrolysis of Fe^{3+} is favorable for the elimination of alcoholic hydroxyl groups rather than the epoxy groups. In this case, the critical pH value when the hydrolysis happens can be indicated from the formation of the red cationic polymer. Since the red precipitates can be observed by human eyes from pH = 0.5, it can be concluded that the critical pH value is around 0.5 in the present system. This rather low pH value is due to the promotion of the hydrolysis reaction by the reaction temperature (95°C). When the pH of FeI_2 solution becomes larger than 0.5, more precipitation of $Fe(OH)_3$ forms between the single-layer rGO sheets, which will further decrease the crystallinity of rGO paper and increase the d_L, as indicated by lower peak height and smaller 2θ value in XRD patterns compared with those of $rGO_{0.5}$. These are responsible for the sharply decreasing of the bulk conductivity of rGO papers. Meanwhile, the ability of H^+ in inhibiting hydrolysis gradually decreases when pH increases. Then, the catalytic effect of strong Lewis acid for the promotion of the nucleophilic substitution reaction of I^- decreases. When the pH is larger than 2, the severe hydrolysis greatly weakens the catalytic effect of strong Lewis acid, hence the conductive ability of FeI_2 becomes inert to pH. As a result, the bulk conductivity of rGO_2 is not much higher than that of rGO_a.

The two pH inert parts on the conductivity curve in Fig. 3a also indicate that the function of H^+ is to inhibit the hydrolysis of FeI_2 rather than to catalyze the nucleophilic substitution reaction. This is consistent with the analysis above.

$$4Fe^{2+} + O_2 + 4H^+ = 4Fe^{3+} + 2H_2O \quad (1)$$

$$Fe^{3+} + H_2O = FeOH^{2+} + H^+ \quad (2)$$

$$FeOH^{2+} + H_2O = Fe(OH)_2^+ + H^+ \quad (3)$$

$$2Fe(OH)_2^+ = Fe_2(OH)_4^{2+} \quad (4)$$

Fig. 6 shows thermogravimetric analysis (TGA) curves of rGO_0, rGO_a, rGO_a immersed in HCl for 48 h, and GO. The GO curve shows a sharp dip at about 200°C, which indicates the decomposing of oxygen containing functional groups[32]. However, for both rGO_0 and rGO_a, such a dip cannot be seen, which is due to the relative high C/O ratio of both rGO_0 and rGO_a, coincident with the result of XPS. Compared with the curve of rGO_0 and GO, the curve of rGO_a shows a wide and mild dip from 100°C to 300°C, which may be due to the evaporation of hydrated water in $Fe(OH)_3{\cdot}(H_2O)_X$ precipitate and the decomposing of $Fe(OH)_3$ precipitate. The curve of rGO_a immersed into hydrochloric acid for 48 hours shows a much less mass loss compared to rGO_a from 100°C to 300°C, indicating that the $Fe(OH)_3$ precipitates are partly eliminated by hydrochloric acid. The TGA results further prove the existence of $Fe(OH)_3{\cdot}(H_2O)_X$ precipitate in the rGO papers. Moreover, it is also noteworthy that the remove of $Fe(OH)_3{\cdot}(H_2O)_X$ precipitate has almost no influence (within standard deviation) on the conductivity of the rGO papers.

The present study shows that FeI_2 acidic solution is a highly efficient, low-cost, mild and environmentally benign reductive agent for the reduction of free-standing GO papers. The rGO papers reduced by FeI_2 acidic solution conferred a bulk conductivity as high as 55088 S/m at low H^+ concentration (pH = 0) and low temperature (95°C). The reductive mechanism is considered as the strong Lewis acid catalyzed nucleophilic substitution reaction. Meanwhile, instead of C/O ratio and defect concentration, the bulk properties of rGO papers, such as crystallinity and d_L, are regarded as the main factors deciding the conductivity of the rGO papers. We believe that the scalable reductive agent presented here may pave the way for a low temperature large-scale synthesis of rGO papers in the future.

Methods

Preparation of GO film. GO was prepared using a modified Hummers' and Offeman's method from natural graphite[25]. A typical experimental procedure is described as follows: A 2 g portion of natural flake graphite (500 mesh), 2 g $NaNO_3$, and 96 mL concentrated H_2SO_4 were mixed at 0°C. During the following stages the mixture was continuously stirred using a magnet stirrer. 12 g $KMnO_4$ was gradually added to the above mixture while keeping the temperature at 0°C. The mixture obtained was first stirred at 0°C for 90 min and then at 35°C for 2 h. Distilled water (80 mL) was slowly dropped into the resulting solution, over a period of around 30 min, to dilute the mixture. Then 200 mL distilled water was added followed by 10 mL of H_2O_2 (30%), and the stirring continued for 10 min to obtain a GO suspension. During this final step, H_2O_2 (30%) reduced the residual permanganate and manganese dioxide to colorless soluble manganese sulfate. The GO deposit was collected from the GO suspension by centrifugation at 4000 rpm for 5 min, and repeatedly washed with distilled water until the pH = 7. Then a sonication (40 W, 1 h) was used to exfoliate the GO to obtain a GO suspension. To obtain uniform single-layer GO sheets, a centrifugation at 4000 rpm for 10 min was used to remove thick multilayer flakes. Then the obtained GO aqueous supernatant was filtered in vacuum to prepare GO paper on mixed cellulose ester filter membrane. After dried at room temperature for 12 hours to remove the remaining water, the GO paper was immersed into acetone to dissolve the mixed cellulose ester filter membrane and to obtain a free-standing GO paper. The AFM image of GO can be obtained from the previous paper reported by our group[26], which proves the fully exfoliation of the GO.

Preparation of metal iodide and reduction of GO papers to rGO papers. Metal iodides (MgI_2, AlI_3, ZnI_2, FeI_2) were synthesized directly from the reaction of iodine/metal powder with some drops of water as a catalyzer. The detailed experimental procedure is described as follows: 5 g iodine particles were pestled into powder in an agate mortar and mixed with 5 g metal powder in a beaker. Then several drops of deionized water were added into the beaker. Soon after that, the reaction between iodine and metal powder fiercely started and ended in 10 seconds. Then the metal iodide was obtained. After that, 200 ml deionized water was added into the beaker, which was stirred until all of the resulting metal iodide was dissolved. Then, the pH value of the supernatant was tuned by adding HCl (1 mol/L) under the measurement of a pH meter. As soon as the critical pH was reached, the supernatant was decanted into another beaker. Finally, the free-standing GO papers were immersed into the supernatant in water bath for 6 h at 95°C to obtain rGO papers. 5 GO samples were reduced at each condition to check the reproducibility and standard deviation of conductivity was obtained.

Characterization. The bulk conductivity of square rGO paper (2 × 2 cm in size) dried under room temperature in air for 12 hours was measured by a digital four-point probe system (SX1934, Suzhou, China). To get reliable bulk conductivity data, four different sites of each sample were measured by the four-point probe system. To get precise thickness of the go papers, the thickness of the rGO paper was observed by a scanning electron microscope (SEM, LEO 1530, Germany) and measured by Tesa probe (Tesa GT21, Swiss). 5 points of each sample were measured and the average thickness was utilized to calculate the conductivity of rGO paper. Raman spectroscopy was performed on a laser micro-Raman spectroscope (Hr800, Horiba Jobin Yvon, France) with a laser beam wavelength of 633 nm. The existing functional groups of GO and rGO were measured by a Fourier-transform infrared spectrometer (FTIR, NICOLET560, Nicolet, USA) with a resolution of 4 cm^{-1}. The X-ray

photoelectron spectroscopy (XPS) spectra were performed on X-ray photoelectron spectrometer (ESCALAB 250 Xi, Thermo SCIENTIFIC, USA) with Al K_α radiation (hv = 1486.6 eV) as source. The crystallinity of RGO papers and layer-to-layer distance (d_L) of rGO sheets was determined by an X-ray diffractometer (XRD, D8 advance, Bruker, Germany), operated at 40 kV and 40 mA. The thermogravimetric analysis was carried out by a thermogravimetric analyzer (STA449F3, NETZSCH, Germany), operated at Ar atmosphere.

1. Roy-Mayhew, J. D., Bozym, D. J., Punckt, C. & Aksay, I. A. Functionalized graphene as a catalytic counter electrode in dye-sensitized solar cells. *ACS Nano* **4**, 6203–6211 (2010).
2. Hu, Y. H., Wang, H. & Hu, B. Thinnest two-dimensional nanomaterial-graphene for solar energy. *Chem. Sus. Chem.* **3**, 782–796 (2010).
3. Xu, Z. W. *et al.* Synthesis of hybrid graphene carbon-coated nanocatalysts. *J. Mater. Chem.* **20**, 8230–8232 (2010).
4. Viet, H. P. *et al.* Chemical functionalization of graphene sheets by solvothermal reduction of a graphene oxide suspension in Nmethyl-2-pyrrolidone. *J. Mater. Chem.* **21**, 3371–3377 (2011).
5. Zhou, X. F., Wang, F., Zhu, Y. M. & Liu, Z. P. Graphene modified $LiFePO_4$ cathode materials for high power lithium ion batteries. *J. Mater. Chem.* **21**, 3353–3358 (2011).
6. Kavan, L. *et al.* Optically transparent cathode for dye-sensitized solar cells based on graphene nanoplatelets. *ACS Nano* **5**, 65–172 (2011).
7. Yen, M. Y. *et al.* Platinum nanoparticles/graphene composite catalyst as a novel composite counter electrode for high performance dye-sensitized solar cells. *J. Mater. Chem.* **21**, 12880–12888 (2011).
8. Zhao, X. *et al.* Carbon nanosheets as the electrode material in supercapacitors. *J. Power Sources.* **194**, 1208–1212 (2009).
9. Bae, J. *et al.* Fiber supercapacitors made of nanowire-fiber hybrid structures for wearable/flexible energy storage. *Angew. Chem. Int. Edit.* **50**, 1683–1687 (2011).
10. Li, Z. P. *et al.* Electrostatic layer-by-layer self-assembly multilayer films based on graphene and manganese dioxide sheets as novel electrode materials for supercapacitors. *J. Mater. Chem.* **21**, 3397–3403 (2011).
11. Liao, L. *et al.* Top-gated graphene nanoribbon transistors with ultrathin high-K dielectrics. *Nano Lett.* **10**, 1917–1921 (2010).
12. Hu, W. *et al.* Graphene-based antibacterial paper. *ACS Nano* **4**, 4317–4323 (2010).
13. Xu, Y. & Shi, G. Assembly of chemically modified graphene: methods and applications. *J. Mater. Chem.* **21**, 3311–3323 (2011).
14. Novoselov, K. S. *et al.* Electric field effect in atomically thin carbon films. *Science* **306**, 666–669 (2004).
15. Bae, S. *et al.* Roll-to-roll production of 30-inch graphene films for transparent electrodes. *Nature Nanotechnology* **5**, 574–578 (2010).
16. Reina, A. *et al.* Large area, few-layer graphene films on arbitrary substrates by chemical vapor deposition. *Nano Lett.* **9**, 30–35 (2009).
17. Dong, X. C. *et al.* Ultra-large single-layer graphene obtained from solution chemical reduction and its electrical properties. *Phys. Chem. Chem. Phys.* **12**, 2164–2169 (2010).
18. Zhou, X. Z. *et al.* In situ synthesis of metal nanoparticles on single-layer graphene oxide and reduced graphene oxide surfaces. *J. Phys. Chem. C.* **113**, 10842–10846 (2009).
19. Zhou, X. F. & Liu, Z. P. A scalable, solution-phase processing route to graphene oxide and graphene ultralarge sheets. *Chem. Commun.* **46**, 2611–2613 (2010).
20. Peng, H., Meng, L. J., Niu, L. Y. & Lu, Q. H. Simultaneous reduction and surface functionalization of graphene oxide by natural cellulose with the assistance of the ionic liquid. *J. Phys. Chem. C.* **116**, 16924–16929 (2012).
21. Mohanty, N., Nagaraja, A., Armesto, J. & Berry, V. High-throughput, ultrafast synthesis of solution-dispersed graphene via a facile hydride chemistry. *Small* **6**, 226–31 (2010).
22. He, F. A. *et al.* The attachment of Fe3O4 nanoparticles to graphene oxide by covalent bonding. *Carbon* **48**, 3139–3144 (2010).
23. Li, J., Lin, H., Yang, Z. & Li, J. A Method for the catalytic reduction of graphene oxide at temperatures below 150°C. *Carbon* **49**, 3024–3030 (2011).
24. Pei, S. F. *et al.* Direct reduction of graphene oxide films into highly conductive and flexible graphene films by hydrohalic acids. *Carbon* **48**, 4466–74 (2010).
25. Zhao, J. P. *et al.* Efficient preparation of large-area graphene oxide sheets for transparent conductive films. *ACS Nano* **4**, 5245–52 (2010).
26. Zhao, X. *et al.* Low-cost preparation of a conductive and catalytic graphene film from chemical reduction with AlI_3. *Carbon* **50**, 3497–3502 (2012).
27. Cancado, L. G. *et al.* Quantifying defects in graphene via raman spectroscopy at different excitation energies. *Nano lett.* **11**, 3190–3196 (2011).
28. Dikin, D. A. *et al.* Preparation and characterization of graphene oxide paper. *Nature* **448**, 457–460 (2007).
29. Bagri, A. *et al.* Structural evolution during the reduction of chemically derived graphene oxide. *Nat. Chem.* **2**, 581–587 (2010).
30. Schniepp, H. C. *et al.* Functionalized single graphene sheets derived from splitting graphite oxide. *J. Phys. Chem. B* **110**, 8535–8539 (2006).
31. Flynn, C. M. Jr. Hydrolysis of inorganic iron (III) salts. *Chem. Rev.* **84**, 31–41 (1984).
32. McAllister, M. J. *et al.* Single Sheet functionalized graphene by oxidation and thermal expansion of Graphite. *Chem. Mater.* **19**, 4396–4404 (2007).

Acknowledgments

The authors would like to express their gratitude for the support provided by the National High Technology Research and Development Program of China (863 Program,2011AA050522), the National Natural Science Foundation of China (NSFC,51272126), and the Ministry of Science & Technology, Israel and the Ministry of Science & Technology, P. R. China: the China-Israel Scientific and Strategic Research Fund (2013DFG53010).

Author contributions

H. Lin conceived the experiments. C. Liu performed the experiments and processed the data. C. Liu, F. Hao, X. Zhao and H. Lin wrote the manuscript. Q. Zhao and S. Luo participated in the synthesis and characterization of the samples. All authors contributed to the review of the manuscript and the discussion of the results.

Additional information

Supplementary information accompanies this paper at http://www.nature.com/scientificreports

Competing financial interests: The authors declare no competing financial interests.

How to cite this article: Liu, C.Y. *et al.* Low temperature reduction of free-standing graphene oxide papers with metal iodides for ultrahigh bulk conductivity. *Sci. Rep.* **4**, 3965; DOI:10.1038/srep03965 (2014).